Synchrony and variability induced by spatially correlated additive and multiplicative noise in the coupled Langevin model

Hideo Hasegawa*
Department of Physics, Tokyo Gakugei University, Koganei, Tokyo 184-8501, Japan
(Received 18 February 2008; revised manuscript received 13 August 2008; published 8 September 2008)

The synchrony and variability of the coupled Langevin model subjected to spatially correlated additive and multiplicative noise are discussed. We have employed numerical simulations and the analytical augmented-moment method, which is the second-order moment method for local and global variables [H. Hasegawa, Phys. Rev. E **67**, 041903 (2003)]. It has been shown that the synchrony of an ensemble is increased (decreased) by a positive (negative) spatial correlation in both additive and multiplicative noise. Although the variability for local fluctuations is almost insensitive to spatial correlations, that for global fluctuations is increased (decreased) by positive (negative) correlations. When a pulse input is applied, the synchrony is increased for the correlated multiplicative noise, whereas it may be decreased for correlated additive noise coexisting with uncorrelated multiplicative noise. An application of our study to neuron ensembles has demonstrated the possibility that information is conveyed by the variance and synchrony in input signals, which accounts for some neuronal experiments.

DOI: 10.1103/PhysRevE.78.031110 PACS number(s): 05.40.Ca, 05.10.Gg, 84.35.+i

I. INTRODUCTION

It has been realized that the coupled Langevin model is a valuable and useful model for a study of various phenomena observed in stochastic ensembles (for a recent review, see Ref. [1]). Independent (uncorrelated) additive and/or multiplicative noise has been widely adopted for theoretical analyses because of its mathematical simplicity. In natural phenomena, however, there exist some kinds of correlations in noise, such as spatial and temporal correlations, and a correlation between additive and multiplicative noise. In this paper we will pay attention to the spatial correlation in noise. The Langevin model has been usually discussed with the use of the Fokker-Planck equation (FPE) for the probability distribution. In the case of correlated additive noise only, the probability distribution is expressed by the multivariate Gaussian probability with a covariance matrix. The effect of correlated additive noise has been extensively studied in neuroscience, where it is an important and essential problem to study the effect of correlations in noise and signals (for a review, see Ref. [2]). It has been shown that the synchrony and variability in neuron ensembles are much influenced by the spatial correlations [3–16]. The spatial correlation in additive noise enhances the synchrony of firings in a neuron ensemble, while it works to diminish beneficial roles of independent noise, such as the stochastic and coherent resonances and the population (pooling) effect [2,10,11,14], related discussions being given in Sec. III.

The problem becomes much difficult when multiplicative noise exists, for which the probability distribution generally becomes a non-Gaussian. Although an analytical expression of the stationary probability distribution for uncorrelated multiplicative noise is available, that for correlated multiplicative noise has not been obtained yet. Indeed, only a small amount of theoretical study of the effect of spatially correlated multiplicative noise has been reported for subjects such as the noise-induced phase separation [17] and the Fisher information [18–20], as far as the author is concerned.

In a recent paper [21], we have studied stationary and dynamical properties of the coupled Langevin model subjected to uncorrelated additive and multiplicative noise. We employed the augmented moment method (AMM), which was developed for a study of stochastic systems with finite populations [22,23]. In the AMM, we consider global properties of ensembles, taking account of mean and fluctuations (variances) of local and global variables. Although a calculation of the probability distribution for the spatially correlated multiplicative noise with the use of the FPE is very difficult as mentioned above, we may easily study its effects by using the AMM. It is the purpose of the present paper to apply the AMM to the coupled Langevin model including spatially correlated multiplicative noise and to study its effects on the synchrony and variability.

The paper is organized as follows. In Sec. II, we discuss the AMM for the spatially correlated Langevin model. With the use of the analytical AMM and numerical methods, the synchrony and variability of the coupled Langevin model are investigated. In Sec. III, previous studies of the correlated multiplicative noise using the Gaussian approximation [18–20] are critically discussed. An application of our study to neuron ensembles is also presented with model calculations. The final Sec. IV is devoted to our conclusion.

II. FORMULATION

A. Adopted model

We have assumed the N-unit coupled Langevin model subjected to spatially correlated additive and multiplicative noise. The dynamics of a variable x_i $(i=1-N)$ is given by

$$\frac{dx_i}{dt} = F(x_i) + H(u_i) + G(x_i)\eta_i(t) + \xi_i(t), \tag{1}$$

with

*hideohasegawa@goo.jp

$$u_i(t) = \left(\frac{w}{Z}\right) \sum_{j(\neq i)} x_j(t) + I_i(t), \tag{2}$$

$$H(u) = \frac{u}{\sqrt{u^2+1}} \Theta(u). \tag{3}$$

Here $F(x)$ and $G(x)$ are arbitrary functions of x, Z $(=N-1)$ denotes the coordination number, $I_i(t)$ an input signal from external sources, w the coupling strength, and $\Theta(u)$ the Heaviside function: $\Theta(u)=1$ for $u>0$ and $\Theta(u)=0$ otherwise. We have included additive and multiplicative noise by $\xi_i(t)$ and $\eta_i(t)$, respectively, expressing zero-mean Gaussian white noise with correlations given by

$$\langle \eta_i(t)\eta_j(t')\rangle = \alpha^2[\delta_{ij} + c_M(1-\delta_{ij})]\delta(t-t'), \tag{4}$$

$$\langle \xi_i(t)\xi_j(t')\rangle = \beta^2[\delta_{ij} + c_A(1-\delta_{ij})]\delta(t-t'), \tag{5}$$

$$\langle \eta_i(t)\xi_j(t')\rangle = 0, \tag{6}$$

where the brackets $\langle\cdot\rangle$ denote the average, α (β) expresses the magnitude of multiplicative (additive) noise, and c_M (c_A) stands for the degree of the spatial correlation in multiplicative (additive) noise. Although our results to be present in the following are valid for any choice of $H(x)$, we have adopted a simple analytic expression given by Eq. (3) in this study.

We assume that external inputs have a variability defined by

$$I_i(t) = I(t) + \delta I_i(t), \tag{7}$$

with

$$\langle \delta I_i(t)\rangle = 0, \tag{8}$$

$$\langle \delta I_i(t)\delta I_j(t')\rangle = \gamma_I[\delta_{ij} + S_I(1-\delta_{ij})]\delta(t-t'), \tag{9}$$

where γ_I and S_I denote the variance and degree of the spatial correlation, respectively, in external signals. We will investigate the response of the coupled Langevin model to correlated external inputs given by Eqs. (7)–(9).

B. Augmented moment method

In the AMM [22,23], we define the three quantities of $\mu(t)$, $\gamma(t)$, and $\rho(t)$ expressed by

$$\mu(t) = \langle X(t)\rangle = \frac{1}{N}\sum_i \langle x_i(t)\rangle, \tag{10}$$

$$\gamma(t) = \frac{1}{N}\sum_i \langle [x_i(t)-\mu(t)]^2\rangle, \tag{11}$$

$$\rho(t) = \langle [X(t)-\mu(t)]^2\rangle, \tag{12}$$

where $X(t)=(1/N)\Sigma_i x_i(t)$, $\mu(t)$ expresses the mean, and $\gamma(t)$ and $\rho(t)$ denote fluctuations in local (x_i) and global variables (X), respectively. By using the FPE, we obtain equations of motion for $\mu(t)$, $\gamma(t)$ and $\rho(t)$ which are given by (argument t is suppressed, details being given in the Appendix A)

$$\frac{d\mu}{dt} = f_0 + h_0 + f_2\gamma + \left(\frac{\alpha^2}{2}\right)[g_0g_1 + 3(g_1g_2 + g_0g_3)\gamma], \tag{13}$$

$$\frac{d\gamma}{dt} = 2f_1\gamma + \frac{2h_1w}{Z}(N\rho-\gamma) + 2(g_1^2 + 2g_0g_2)\alpha^2\gamma + \gamma_I + \beta^2 + \alpha^2 g_0^2, \tag{14}$$

$$\frac{d\rho}{dt} = 2f_1\rho + 2h_1w\rho + 2(g_1^2 + 2g_0g_2)\alpha^2\rho + \frac{1}{N}(\gamma_I + \beta^2 + \alpha^2 g_0^2) + \frac{Z}{N}(S_I\gamma_I + c_A\beta^2 + c_M\alpha^2 g_0^2), \tag{15}$$

where $f_\ell=(1/\ell!)[\partial^\ell F(\mu)/\partial x^\ell]$, $g_\ell=(1/\ell!)[\partial^\ell G(\mu)/\partial x^\ell]$, $h_\ell=(1/\ell!)[\partial^\ell H(u)/\partial u^\ell]$, and $u=w\mu+I$. Original N-dimensional stochastic differential equations (DEs) given by Eqs. (1)–(3) are transformed to the three-dimensional deterministic DEs given by Eqs. (13)–(15). For $\gamma_I=S_I=c_A=c_M=0$, equations of motion given by Eqs. (13)–(15) reduce to those obtained in our previous study [21].

When we adopt $F(x)$ and $G(x)$ given by

$$F(x) = -\lambda x, \tag{16}$$

$$G(x) = x, \tag{17}$$

Eqs. (13)–(15) become

$$\frac{d\mu}{dt} = -\lambda\mu + h_0 + \frac{\alpha^2\mu}{2}, \tag{18}$$

$$\frac{d\gamma}{dt} = -2\lambda\gamma + \frac{2h_1wN}{Z}\left(\rho - \frac{\gamma}{N}\right) + 2\alpha^2\gamma + P, \tag{19}$$

$$\frac{d\rho}{dt} = -2\lambda\rho + 2h_1w\rho + 2\alpha^2\rho + \frac{(P+ZR)}{N}, \tag{20}$$

with

$$P = \gamma_I + \beta^2 + \alpha^2\mu^2, \tag{21}$$

$$R = S_I\gamma_I + c_A\beta^2 + c_M\alpha^2\mu^2, \tag{22}$$

where $h_0=H(w\mu+I)$, and P and R express uncorrelated and correlated contributions, respectively. We employ Eqs. (18)–(22) in the remainder of this paper.

C. Synchrony and variability

1. Synchrony

In order to quantitatively discuss the synchronization, we first consider the quantity $S'(t)$ given by

$$S'(t) = \frac{1}{N^2}\sum_{ij}\langle [x_i(t)-x_j(t)]^2\rangle = 2[\gamma(t)-\rho(t)]. \tag{23}$$

When all neurons are in the same state, $x_i(t)=X(t)$ for all i (the completely synchronous state), we obtain $S'(t)=0$ in Eq.

(23). On the contrary, in the asynchronous state where $\rho = \gamma/N$, it is given by $S'(t)=2(1-1/N)\gamma(t)\equiv S'_0(t)$ [21,22]. We may define the normalized ratio for the synchrony given by [22,23]

$$S(t) \equiv 1 - \frac{S'(t)}{S'_0(t)} = \left(\frac{N}{Z}\right)\left(\frac{\rho(t)}{\gamma(t)} - \frac{1}{N}\right), \tag{24}$$

which is 0 and 1 for completely asynchronous ($S'=S'_0$) and synchronous states ($S'=0$), respectively.

2. Variability

The local variability is conventionally given by

$$C_V(t) = \frac{\sqrt{\langle[\delta x_i(t)]^2\rangle}}{\mu(t)} = \frac{\sqrt{\gamma(t)}}{\mu(t)}, \tag{25}$$

where $\delta x_i(t)=x_i(t)-\mu(t)$. Similarly, the global variability is defined by

$$D_V(t) = \frac{\sqrt{\langle[\delta X(t)]^2\rangle}}{\mu(t)} = \frac{\sqrt{\rho(t)}}{\mu(t)} = C_V(t)\sqrt{\frac{\rho(t)}{\gamma(t)}}, \tag{26}$$

where $\delta X(t)=X(t)-\mu(t)$.

D. Stationary properties

The stationary solution of Eqs. (18)–(20) is given by

$$\mu = \frac{h_0}{(\lambda - \alpha^2/2)}, \tag{27}$$

$$\gamma = \frac{P}{2(\lambda - \alpha^2 + h_1 w/Z)} + \frac{(h_1 w/Z)(P+ZR)}{2(\lambda - \alpha^2 + h_1 w/Z)(\lambda - \alpha^2 - h_1 w)}, \tag{28}$$

$$\rho = \frac{P+ZR}{2N(\lambda - \alpha^2 - h_1 w)}, \tag{29}$$

where μ in P and R of Eqs. (21) and (22) is given by Eq. (27). We note in Eq. (27) that μ is increased as I is increased with an enhancement factor of $1/(\lambda-\alpha^2/2)$. A local fluctuation γ is increased with increasing input fluctuations (γ_I) and/or noise (α,β) as Eq. (28) shows. In the limit of $S_I=c_A=c_M=R=w=0.0$, Eqs. (28) and (29) lead to $\rho/\gamma=1/N$, which expresses the central-limit theorem. From Eqs. (24), (28), and (29), we obtain

$$S = \frac{h_1 wP + Z(\lambda - \alpha^2)R}{P[Z(\lambda - \alpha^2) - h_1 w(Z-1)] + h_1 wZR} \tag{30}$$

$$= \frac{h_1 w}{Z(\lambda - \alpha^2) - h_1 w(Z-1)} \quad (\text{for } S_I = c_A = c_M = 0) \tag{31}$$

$$= \frac{S_I\gamma_I + c_A\beta^2 + c_M\alpha^2\mu^2}{\gamma_I + \beta^2 + \alpha^2\mu^2} \quad (\text{for } w=0), \tag{32}$$

where P and R in Eq. (30) are given by Eqs. (21) and (22), respectively. Equation (30) shows that the synchrony S is increased with increasing spatial correlations and/or coupling. This is more clearly seen in the limit of no spatial correlations [Eq. (31)] or no couplings [Eq. (32)]. The local and global variabilities C_V and D_V defined by Eqs. (25) and (26), respectively, are generally expressed in terms of P and R, and they are given for $w=0.0$ by

$$C_V = \frac{1}{\mu}\left(\frac{\gamma_I + \beta^2 + \alpha^2\mu^2}{2(\lambda - \alpha^2)}\right)^{1/2} \quad \text{for } w=0, \tag{33}$$

$$D_V = C_V\left(\frac{(1+ZS_I)\gamma_I + (1+Zc_A)\beta^2 + (1+Zc_M)\alpha^2\mu^2}{N(\gamma_I + \beta^2 + \alpha^2\mu^2)}\right)^{1/2} \quad \text{for } w=0. \tag{34}$$

The local variability C_V only weakly depends on the spatial correlation through the coupling, and it is independent of the correlation for $w=0$. In contrast, the global variability D_V is increased (decreased) for positive (negative) correlations. In the limit of $S_I=c_A=c_M=w=0.0$, Eq. (34) yields $D_V=C_V/\sqrt{N}$ expressing a smaller global variability in a larger-N ensemble (the population or pooling effect) [2,10,11,14].

The stability condition around the stationary state given by Eqs. (27)–(29) may be examined from eigenvalues of the Jacobian matrix of Eqs. (18)–(20), which are given by

$$\lambda_1 = -\lambda + \frac{\alpha^2}{2} + h_1 w, \tag{35}$$

$$\lambda_2 = -2\lambda + 2\alpha^2 - \frac{2h_1 w}{Z}, \tag{36}$$

$$\lambda_3 = -2\lambda + 2\alpha^2 + 2h_1 w. \tag{37}$$

The first eigenvalue of λ_1 arises from an equation of motion for μ, which is decoupled from the rest of variables. The stability condition for μ is given by

$$h_1 w < (\lambda - \alpha^2/2). \tag{38}$$

The stability condition for γ and ρ is given by

$$-Z(\lambda - \alpha^2) < h_1 w < (\lambda - \alpha^2). \tag{39}$$

Then for $\lambda-\alpha^2<h_1w<\lambda-\alpha^2/2$, γ and ρ are unstable, but μ remains stable.

It is note that there is a limitation in a parameter value of c, as given by

$$-\frac{1}{Z} \leqslant \left(\frac{S_I\gamma_I + c_A\beta^2 + c_M\alpha^2\mu^2}{\gamma_I + \beta^2 + \alpha^2\mu^2}\right) \leqslant 1, \tag{40}$$

which arises from the condition given by $0\leqslant\rho\leqslant\gamma$ [see Eqs. (12) and (23)]. When $\beta=\gamma_I=0$, for example, a physically conceivable value of c_M is given by $-1/Z\leqslant c_M\leqslant 1$.

The c_M dependence of the synchrony S is shown in Fig. 1 where $\alpha=0.1$, $\beta=0.1$, $c_A=0.1$, $\gamma_I=S_I=0$, and $N=100$. Equation (40) yields the condition that $-0.44<c_M<1.0$ with $\mu=0.5$ for a given set of parameters. We note that the synchrony is increased with increasing s and that the effect of the correlated variability is more considerable for larger μ and w, as Eq. (30) shows.

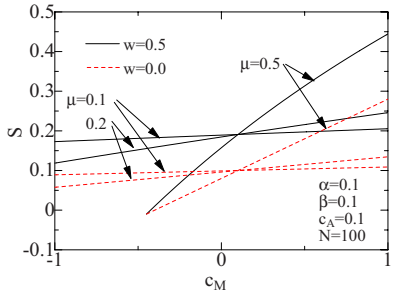

FIG. 1. (Color online) c_M dependence of the stationary synchrony S for $w=0.5$ (solid curves) and $w=0.0$ (dashed curves) with $\alpha=0.1$, $\beta=0.1$, $c_A=0.1$, $\gamma_I=S_I=0$, and $N=100$, μ being treated as a parameter.

E. Dynamical properties

In order to study the dynamical properties of our model given by Eqs. (1)–(3), we have performed direct simulations (DSs) by using the Heun method [24,25] with a time step of 0.0001: DS results are averages of 100 trials. AMM calculations have been performed for Eqs. (18)–(20) by using the fourth-order Runge-Kutta method with a time step of 0.01. We consider a set of typical parameters of $\lambda=1.0$, $\alpha=0.1$, $\beta=0.1$, $w=0.5$, $\gamma_I=S_I=0$, and $N=100$. We apply a pulse input given by

$$I(t) = A\Theta(t-40)\Theta(60-t) + A_b, \tag{41}$$

with $A=0.4$ and $A_b=0.1$, where $\Theta(x)$ denotes the Heaviside function: $\Theta(x)=1$ for $x \geqslant 0$ and 0 otherwise.

Figures 2(a)–2(d) show time courses of $\mu(t)$, $\gamma(t)$, $S(t)$, and $C_V(t)$ for the correlated multiplicative noise ($c_A=0.0$ and $c_M=0.5$). $\mu(t)$ and $S(t)$ are increased by an applied input at $40 \leqslant t < 60$ shown by the chain curve in Fig. 2(a), by which $\gamma(t)$ is slightly increased. The variability $C_V(t)$ is decreased because of an increased $\mu(t)$. The results of the AMM shown by the solid curves are in fairly good agreement with those of DSs shown by the dashed curves.

In contrast, Figs. 3(a)–3(d) show time courses of $\mu(t)$, $\gamma(t)$, $S(t)$, and $C_V(t)$ for the correlated additive noise ($c_A=0.1$ and $c_M=0.0$). With an applied pulse input, $\mu(t)$ is increased and $\gamma(t)$ is a little increased, as in the case of Figs. 2(a) and 2(b). However, the synchrony $S(t)$ is decreased in Fig. 3(c), while it is increased in Fig. 2(c). This difference arises from the fact that a decrease in $S(t)$ in the former case is mainly due to an increase in P of the denominator of Eq. (30), while in the latter case, its increase arises from an increase in R of the numerator of Eq. (30). This point is more easily realized for $w=0$, for which Eq. (32) yields

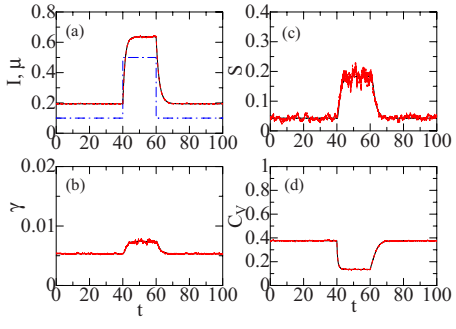

FIG. 2. (Color online) Time courses of (a) $\mu(t)$, (b) $\gamma(t)$, (c) $S(t)$, and (d) $C_V(t)$ with the correlated multiplicative noise ($c_A=0.0$, $c_M=0.5$, $\alpha=0.1$, $\beta=0.1$) for a pulse input given by Eq. (41) with $A=0.4$ and $A_b=0.1$: the solid and dotted curves express results of the AMM and DS, respectively: the chain curve in (a) expresses an input of $I(t)$ ($\lambda=1.0$, $S_I=\gamma_I=0.0$, and $N=100$).

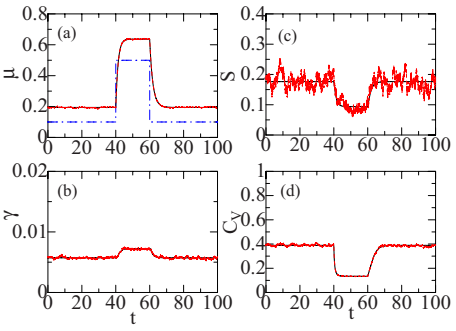

FIG. 3. (Color online) Time courses of (a) $\mu(t)$, (b) $\gamma(t)$, (c) $S(t)$, and (d) $C_V(t)$ with the correlated additive noise ($c_A=0.1$, $c_M=0.0$, $\alpha=0.1$, $\beta=0.1$) for a pulse input given by Eq. (41) with $A=0.4$ and $A_b=0.1$: the solid and dashed curves denote results of the AMM and DSs, respectively: the chain curve in (a) expresses an input of $I(t)$ ($\lambda=1.0$, $S_I=\gamma_I=0.0$, and $N=100$).

$$S = \frac{c_M \alpha^2 \mu^2}{\beta^2 + \alpha^2 \mu^2} \quad (\text{for } c_A = 0) \tag{42}$$

$$= \frac{c_A \beta^2}{\beta^2 + \alpha^2 \mu^2} \quad (\text{for } c_M = 0). \tag{43}$$

The situation is almost the same even for finite w, as Figs. 2(c) and 3(c) show. In both Figs. 2(d) and 3(d), $C_V(t)$ is decreased by an applied input because of an increased $\mu(t)$.

III. DISCUSSION

A. Comparison with related studies

We have investigated the stationary and dynamical properties of the spatially correlated Langevin model given by Eqs. (1)–(3). In Ref. [26], we discussed the Fisher information in the Langevin model subjected to uncorrelated additive and multiplicative noise, which is a typical microscopic model showing the nonextensive behavior [27]. It is interesting to calculate the Fisher information of the Langevin model with correlated multiplicative noise. Such a calculation needs to solve the FPE of the Langevin model given by Eq. (A1) because the Fisher information is expressed in terms of derivatives of the probability distribution. For additive noise only ($\alpha=c_M=0$), the stationary probability distribution $p(\{x_k\})$ is expressed by the multivariate Gaussian distribution given by

$$p(\{x_k\}) \propto \exp\left[-\frac{1}{2} \sum_{ij} (x_i - \mu)(\mathsf{Q}^{-1})_{ij} (x_j - \mu) \right], \tag{44}$$

with the covariance matrix Q expressed by

$$Q_{ij} = \sigma^2[\delta_{ij} + c_A(1 - \delta_{ij})], \tag{45}$$

where $\mu = H/\lambda$ and $\sigma^2 = \beta^2/2\lambda$. From Eqs. (44) and (45), we obtain the Fisher information given by [18]

$$g = \frac{N}{\sigma^2[1 + (N-1)c_A]}. \tag{46}$$

When multiplicative noise exists, a calculation of even stationary distribution becomes difficult, and it is generally not given by the Gaussian. The stationary distribution for *uncorrelated* additive and multiplicative noise [$G(x)=x$, $c_A = c_M = \gamma_I = 0.0$] is given by [21,26,28,29]

$$p(\{x_k\}) \propto \prod_i (\beta^2 + \alpha^2 x_i^2)^{-(\alpha^2/\lambda + 1/2)} e^{(2H/\alpha\beta)\tan^{-1}(\alpha x_i/\beta)}. \tag{47}$$

In the limit of $\alpha = 0.0$ and $\beta \neq 0.0$ (i.e., uncorrelated additive noise only), Eq. (47) becomes the Gaussian distribution given by

$$p(\{x_k\}) \propto \prod_i e^{-(\lambda/\beta^2)(x_i - \mu)^2}. \tag{48}$$

In the opposite limit of $\alpha \neq 0.0$, $\beta = 0.0$, and $H > 0$ (i.e., uncorrelated multiplicative noise only), Eq. (47) reduces to

$$p(\{x_k\}) \propto \prod_i x_i^{-(2\alpha^2/\lambda + 1)} e^{-2H/\alpha^2 x_i} \Theta(x_i), \tag{49}$$

yielding the Fisher information given by

$$g = \frac{Nq^4}{\sigma_q^2} = \frac{2N\lambda q^4}{\alpha^2 \mu^2}, \tag{50}$$

where $q = (2\lambda + 3\alpha^2)/(2\lambda + \alpha^2)$ and $\sigma_q^2 = \alpha^2\mu^2/2\lambda$ [26].

Unfortunately, we have not succeeded in obtaining the analytic expression for the stationary distribution of the Langevin model including *correlated* multiplicative noise. In some previous studies [18–20], the stationary distribution for correlated multiplicative noise only ($G(x)=x$, $c_A = \beta = 0.0$, and $H = \mu$) is assumed to be expressed by the Gaussian distribution given by Eq. (44) with the covariance matrix given by

$$Q_{ij} = \sigma_M^2 \mu_i \mu_j [\delta_{ij} + c_M(1 - \delta_{ij})], \tag{51}$$

where μ_i ($=\langle x_i \rangle$) denotes the average of x_i and σ_M^2 a variance due to multiplicative noise. This is equivalent to assume that the multiplicative-noise term in the FPE given by Eq. (A1) is approximated as

$$\begin{aligned} &\frac{\alpha^2}{2} \sum_i \sum_j [\delta_{ij} + c_M(1 - \delta_{ij})] \frac{\partial}{\partial x_i} x_i \frac{\partial}{\partial x_j} x_j p(\{x_k\}) \\ &\simeq \frac{\alpha^2}{2} \sum_i \sum_j [\delta_{ij} + c_M(1 - \delta_{ij})] \frac{\partial}{\partial x_i} \langle x_i \rangle \frac{\partial}{\partial x_j} \langle x_j \rangle p(\{x_k\}) \\ &= \frac{\alpha^2}{2} \sum_j \sum_i \mu_i \mu_j [\delta_{ij} + c_M(1 - \delta_{ij})] \frac{\partial}{\partial x_i} \frac{\partial}{\partial x_j} p(\{x_k\}). \end{aligned} \tag{52}$$

If we adopt the Gaussian approximation given by Eq. (52), with which multiplicative noise may be treated in the same way as additive noise, we obtain the AMM equations given by Eqs. (18)–(20), but without the third term of $\alpha^2\mu/2$ in Eq. (18).

By using the Gaussian approximation given by Eq. (51), Abbott and Dayan (AD) [18] obtained the Fisher information expressed by [Eq. 4.7 of Ref. [18]]

$$g_{AD} = \frac{NK}{\sigma_M^2[1 + (N-1)c_M]} + 2NK \tag{53}$$

$$= \frac{1}{\sigma_M^2 \mu^2 c_M} + \frac{2N}{\mu^2} \quad (\text{for } N \to \infty) \tag{54}$$

$$= \frac{N}{\sigma_M^2 \mu^2} + \frac{2N}{\mu^2} \quad (\text{for } c_M = 0), \tag{55}$$

with $K = N^{-1}\Sigma_i [d \ln H(\mu_i)/d\mu_i]^2 = 1/\mu^2$. Equation (55) is not in agreement with the exact expression given by Eq. (50) for uncorrelated multiplicative noise only.

Instead of using the Langevin model, we may alternatively calculate the Fisher information of a spatially correlated nonextensive system by using the maximum-entropy method. In our recent paper [30], we have obtained the analytic, stationary probability distribution which maximizes the Tsallis entropy [27] under the constraints for a given set of the variance (σ^2) and covariance ($c\sigma^2$). The Fisher information is expressed by [30]

$$g = \frac{N}{\sigma^2[1 + (N-1)c]} \tag{56}$$

$$= \frac{1}{c\sigma^2} \quad (\text{for } N \to \infty) \tag{57}$$

$$= \frac{N}{\sigma^2} \quad (\text{for } c = 0.0). \tag{58}$$

The Fisher information given by Eq. (56) is increased (decreased) by a negative (positive) correlation. This implies from the Cramér-Rao theorem that an unbiased estimate of fluctuations is improved by a negative spatial correlation, by which the synchrony is decreased as shown by Eqs. (30) and (32). The N and c dependences of the Fisher information given by Eq. (56) are different from those of g_{AD} given by Eq. (53), although they are the same as those for additive noise only [Eq. (46)]. It is noted that the Gaussian approximation given by Eq. (51) or (52) assumes the Gaussian distribution, although multiplicative noise generally yields the non-Gaussian distribution as shown by Eqs. (47) and (49). The spurious second term ($2NK$) in Eq. (53), which is independent of c_M and σ_M^2, arises from an inappropriate Gaussian approximation. In discussing the Fisher information of spatially correlated nonextensive systems, we must take into account the detailed structure of the non-Gaussian distribution.

B. Application to neuronal ensembles

When γ_I and S_I in Eq. (9) are allowed to be time dependent, they may carry input information. This is easily real-

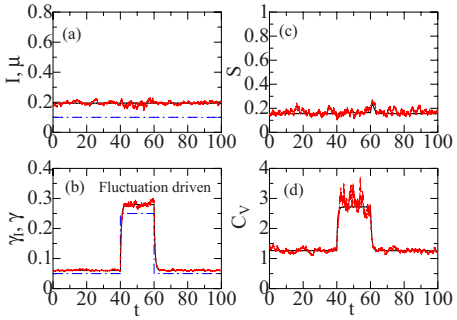

FIG. 4. (Color online) Time courses of (a) $\mu(t)$, (b) $\gamma(t)$, (c) $S(t)$, and (d) $C_V(t)$ for a fluctuation-driven input of $\gamma_I(t)$ given by Eq. (62) with S_I=0.1, B=0.4, and B_b=0.1: the solid and dotted curves express results of the AMM and DS, respectively: the chain curves in (a) and (b) express inputs of $I(t)$ and $\gamma_I(t)$, respectively (λ=1.0, c_A=0.0, c_M=0.5, α=0.1, β=0.1, N=100).

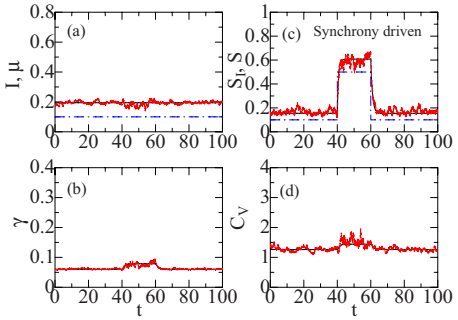

FIG. 5. (Color online) Time courses of (a) $\mu(t)$, (b) $\gamma(t)$, (c) $S(t)$, and (d) $C_V(t)$ for a synchrony-driven input of $S_I(t)$ given by Eq. (63) with γ_I=0.1, C=0.4, and C_b=0.1: the solid and dotted curves express results of the AMM and DS, respectively: the chain curves in (a) and (c) express inputs of $I(t)$ and $S_I(t)$, respectively (λ=1.0, c_A=0.0, c_M=0.5, α=0.1, β=0.1, N=100).

ized if the AMM equations given by Eqs. (18)–(20) are explicitly expressed in terms of μ, γ, and S as

$$\frac{d\mu}{dt} = -\lambda\mu + h_0 + \frac{\alpha^2\mu}{2}, \tag{59}$$

$$\frac{d\gamma}{dt} = -2\lambda\gamma + 2h_1 w\gamma S + 2\alpha^2\gamma + \gamma_I(t) + \alpha^2\mu^2 + \beta^2, \tag{60}$$

$$\frac{dS}{dt} = -\frac{S}{\gamma}[\gamma_I(t) + \alpha^2\mu^2 + \beta^2] + \frac{1}{\gamma}[\gamma_I(t)S_I(t) + c_M\alpha^2\mu^2 + c_A\beta^2] + \left(\frac{2h_1 w}{Z}\right)(1+ZS)(1-S), \tag{61}$$

which are derived with the use of Eq. (24).

In order to numerically examine the possibility that input information is conveyed by $\gamma_I(t)$ and $S_I(t)$, we first apply a fluctuation-driven input given by

$$\gamma_I(t) = B\Theta(t-40)\Theta(60-t) + B_b, \tag{62}$$

with B=0.4, B_b=0.1, $I(t)$=0.1, and $S_I(t)$=0.1 for λ=1.0, c_A=0.0, c_M=0.5, α=0.1, β=0.1, and N=100. Time courses of $\mu(t)$, $\gamma(t)$, $S(t)$, and $C_V(t)$ are shown in Figs. 4(a)–4(d): the chain curves in Figs. 4(a) and 4(b) express $I(t)$ and $\gamma_I(t)$, respectively. When the magnitude of $\gamma_I(t)$ is increased at $40 \leqslant t < 60$, $\gamma(t)$ and $C_V(t)$ are much increased, while there is no changes in $\mu(t)$ because it is decoupled from the rest of variables in Eq. (18). $S(t)$ is slightly modified only at $t \sim 40$ and $t \sim 60$ where the $\gamma_I(t)$ is on and off.

Next we apply a synchrony-driven input $S_I(t)$ given by

$$S_I(t) = C\Theta(t-40)\Theta(60-t) + C_b, \tag{63}$$

with C=0.4, C_b=0.1, $I(I)$=0.1, and $\gamma_I(t)$=0.1. Figures 5(a)–5(d) show time courses of $\mu(t)$, $\gamma(t)$, $S(t)$, and $C_V(t)$: the chain curves in Figs. 5(a) and 5(c) express $I(t)$ and $S_I(t)$, respectively. An increase in synchrony-driven input at $40 \leqslant t < 60$ induces a significant increase in $S(t)$ and slight increases in $\gamma(t)$ and $C_V(t)$, but no changes in $\mu(t)$.

When we regard a variable x_i in the Langevin model given by Eqs. (1)–(3) as the firing rate r_i (>0) of a neuron i in a neuron ensemble, our model expresses the neuronal model proposed in Refs. [31,32]. It belongs to the firing-rate (rate-code) models such as the Wilson-Cowan [33] and Hopfield models [34], in which a neuron is regarded as a transducer from input rate signals to output rate ones. Alternative neuronal models are spiking-neuron (temporal-code) models such as the Hodgkin-Huxley [35], FitzHugh-Nagumo [36,37], and integrate-and-fire (IF) models [38]. Various attempts have been proposed to obtain the firing-rate model, starting from spiking-neuron models [39–43]. It is difficult to analytically calculate the firing rate based on spiking-neuron models, except for the IF-type model [38]. It has been shown with the use of the IF model that information transmission is possible by noise-coded signals [44,45] and that the modulation of the synchrony is possible without a change in firing rate [46]. Model calculations shown in Figs. 4 and 5 have demonstrated the possibility that information may be conveyed by $\gamma_I(t)$ and $S_I(t)$, which is partly supported by results of the IF model [44–46]. Some relevant results have been reported in neuronal experiments [47–52]. In motor tasks of monkey, firing rate and synchrony are considered to encode behavioral events and cognitive events, respectively [47]. During visual tasks, rate and synchrony are suggested to encode task-related signals and expectation, respectively [48]. A change in synchrony may amplify behaviorally relevant signals in V4 of monkeys [49]. The synchrony is modified without a change in firing rate in some experiments [47,49,51]. The synchrony-dependent firing-rate signal is shown to propagate in iteratively constructed networks *in vitro* [50].

IV. CONCLUSION

With the use of DSs and the AMM [22,23], the effects of spatially correlated additive and multiplicative noise have been discussed on the synchrony and variability in the coupled Langevin model. Our calculations have shown the following: (i) the synchrony is increased (decreased) by the positive (negative) correlation in additive and multiplicative

noise [Eq. (30)], (ii) although an applied pulse input works to increase the synchrony for correlated multiplicative noise, it is possible to decrease the synchrony when correlated additive noise coexists with uncorrelated multiplicative one, (iii) the local variability C_V is almost independent of spatial correlations, while global variability D_V is increased (decreased) with increasing the positive (negative) correlation, and (iv) information may be carried by variance and synchrony in input signals. Item (iv) is consistent with the results of Refs. [44–46] and elucidates some phenomena observed in neuronal experiments [47–52].

Although we have applied the AMM to the Langevin model in this paper, it is possible to apply it to other types of stochastic neuronal models such as the FitzHugh and Hodgkin-Huxley models subjected to correlated additive and multiplicative noise, which is left as our future study.

ACKNOWLEDGMENT

This work is partly supported by a Grant-in-Aid for Scientific Research from the Japanese Ministry of Education, Culture, Sports, Science and Technology.

APPENDIX: DERIVATION OF THE AMM EQUATIONS

The FPE for the Langevin equation given by Eqs. (1)–(3) in the Stratonovich representation is expressed by [17,53]

$$\frac{\partial}{\partial t}p(\{x_k\},t) = -\sum_i \frac{\partial}{\partial x_i}\{[F(x_i)+H(u_i)]p(\{x_k\},t)\} + \frac{\gamma_I}{2}\sum_i\sum_j \frac{\partial^2}{\partial x_i \partial x_j}\{[\delta_{ij}+S_I(1-\delta_{ij})]p(\{x_k\},t)\} + \frac{\beta^2}{2}\sum_i\sum_j \frac{\partial^2}{\partial x_i \partial x_j}\{[\delta_{ij}+c_A(1-\delta_{ij})]p(\{x_k\},t)\} + \frac{\alpha^2}{2}\sum_i\sum_j [\delta_{ij}+c_M(1-\delta_{ij})] \times \frac{\partial}{\partial x_i}\left\{G(x_i)\frac{\partial}{\partial x_j}[G(x_j)p(\{x_k\},t)]\right\}, \tag{A1}$$

where $u_i=(w/Z)\Sigma_{j(\neq i)}x_j+I$ and $H'(u_i)$ is absorbed in a new definition of γ_I in its second term.

Equations of motion for moments $\langle x_i\rangle$ and $\langle x_i x_j\rangle$ are derived with the use of the FPE [21]:

$$\frac{d\langle x_i\rangle}{dt} = \langle F(x_i)+H(u_i)\rangle + \frac{\alpha^2}{2}\langle G'(x_i)G(x_i)\rangle, \tag{A2}$$

$$\frac{d\langle x_i x_j\rangle}{dt} = \langle x_i[F(x_j)+H(u_j)]\rangle + \langle x_j[F(x_i)+H(u_i)]\rangle + \frac{\alpha^2}{2}[\langle x_i G'(x_j)G(x_j)\rangle + \langle x_j G'(x_i)G(x_i)\rangle] + \delta_{ij}[\gamma_I+\beta^2+\alpha^2\langle G(x_i)^2\rangle] + (1-\delta_{ij})[S_I\gamma_I + c_A\beta^2 + c_M\alpha^2\langle G(x_i)G(x_j)\rangle]. \tag{A3}$$

In the AMM [22,23], the three quantities of μ, γ, and ρ are defined by Eqs. (10)–(12). We use the expansion given by

$$x_i = \mu + \delta x_i \tag{A4}$$

and the relations given by

$$\frac{d\mu}{dt} = \frac{1}{N}\sum_i \frac{d\langle r_i\rangle}{dt}, \tag{A5}$$

$$\frac{d\gamma}{dt} = \frac{1}{N}\sum_i \frac{d\langle(\delta r_i)^2\rangle}{dt}, \tag{A6}$$

$$\frac{d\rho}{dt} = \frac{1}{N^2}\sum_i\sum_j \frac{d\langle \delta r_i \delta r_j\rangle}{dt}. \tag{A7}$$

For example, Eq. (A5) for $d\mu/dt$ is calculated as follows:

$$\frac{1}{N}\sum_i \langle F(r_i)\rangle = f_0 + f_2\gamma, \tag{A8}$$

$$\frac{1}{N}\sum_i \langle H(u_i)\rangle = h_0, \tag{A9}$$

$$\frac{1}{N}\sum_i \langle G'(r_i)G(r_i)\rangle = g_0 g_1 + 3(g_0 g_3 + g_1 g_2)\gamma. \tag{A10}$$

Equations (A6) and (A7) are calculated in a similar way. Then, we have obtained equations of motion for $\mu(t)$, $\gamma(t)$, and $\rho(t)$ given by Eqs. (13)–(15).

[1] B. Lindner, J. Garcia-Ojalvo, A. Neiman, and L. Schimansky-Geier, Phys. Rep. **392**, 321 (2004).
[2] B. B. Averbeck, P. E. Latham, and A. Pouget, Nat. Rev. Neurosci. **358**, 358 (2006).
[3] A. N. Burkitt and G. M. Clark, Neural Comput. **11**, 871 (1999).
[4] D. Chawla, E. D. Lumer, and K. J. Friston, Neural Comput. **11**, 1389 (1999).
[5] J. Feng and D. Brown, Neural Comput. **12**, 671 (2000).
[6] S. M. Bohte, H. Spekreijse, and P. R. Roelfsema, Neural Comput. **12**, 153 (2000).
[7] S. Stroeve and S. Gielen, Neural Comput. **13**, 2005 (2001).
[8] J. Feng and P. Zhang, Phys. Rev. E **63**, 051902 (2001).
[9] A. Kuhn, S. Rotter, and A. Aertsen, Neurocomputing **44-46**, 121 (2002).
[10] F. Liu, B. Hu, and W. Wang, Phys. Rev. E **63**, 031907 (2001).
[11] S. Wang, F. Liu, W. Wang, and Y. Yu, Phys. Rev. E **69**, 011909 (2004).

[12] B. Doiron, B. Lindner, A. Longtin, L. Maler, and J. Bastian, Phys. Rev. Lett. **93**, 048101 (2004).
[13] B. Lindner, B. Doiron, and A. Longtin, Phys. Rev. E **72**, 061919 (2005).
[14] O. Kwon, H.-H. Jo, and H.-T. Moon, Phys. Rev. E **72**, 066121 (2005).
[15] J. de la Rocha, B. Doiron, E. Shea-Brown, K. Josić, and A. Reyes, Nature (London) **448**, 802 (2007).
[16] E. Shea-Brown, K. Josić, J. dela Rocha, and B. Doiron, Phys. Rev. Lett. **100**, 108102 (2008).
[17] M. Ibanes, J. Garcia-Ojalvo, R. Toral, and J. M. Sancho, Phys. Rev. E **60**, 3597 (1999).
[18] L. F. Abbott and P. Dayan, Neural Comput. **11**, 91 (1999).
[19] S. D. Wilke and C. W. Eurich, Neurocomputing **44-46**, 1023 (2002).
[20] S. Wu, S. Amari, and H. Nakamura, Neural Networks **17**, 205 (2004).
[21] H. Hasegawa, Physica A **374**, 585 (2007).
[22] H. Hasegawa, Phys. Rev. E **67**, 041903 (2003).
[23] H. Hasegawa, J. Phys. Soc. Jpn. **75**, 033001 (2006).
[24] In the Heun method for the ordinary differential equation of $dx/dt=f(x)$, a value of x at $t+h$ is evaluated by $x(t+h)=x(t)+(h/2)[f(x_0)+f(x_1)]$ with $x_0=x(t)$ and $x_1=x(t)+hf(x(t))$, while it is given by $x(t+h)=x(t)+hf(x(t))$ in the Euler method, h being the time step. The Heum method for the stochastic ordinary differential equation meets the Stratonovich calculus employed in the FPE [25].
[25] W. Rümelin, SIAM (Soc. Ind. Appl. Math.) J. Numer. Anal. **19**, 604 (1982); A. Greiner, W. Strittmatter, and J. Honerkamp, J. Stat. Phys. **51**, 95 (1988); R. F. Fox, I. R. Gatland, R. Roy, and G. Vemuri, Phys. Rev. A **38**, 5938 (1988).
[26] H. Hasegawa, Phys. Rev. E **77**, 031133 (2008).
[27] C. Tsallis, J. Stat. Phys. **52**, 479 (1988); C. Tsallis, R. S. Mendes, and A. R. Plastino, Physica A **261**, 534 (1998); C. Tsallis, Physica D **193**, 3 (2004).
[28] H. Sakaguchi, J. Phys. Soc. Jpn. **70**, 3247 (2001).
[29] C. Anteneodo and C. Tsallis, J. Math. Phys. **44**, 5194 (2003).
[30] H. Hasegawa, Phys. Rev. E **78**, 021141 (2008).
[31] H. Hasegawa, Phys. Rev. E **75**, 051904 (2007).
[32] H. Hasegawa, in *Neuronal Network Research Horizons*, edited by M. L. Weiss (Nova Science Publishers, New York, 2007), p. 61; NeuroQuantology **6**, 105 (2008).
[33] H. R. Wilson and J. D. Cowan, Biophys. J. **12**, 1 (1972).
[34] J. J. Hopfield, Proc. Natl. Acad. Sci. U.S.A. **79**, 2554 (1982).
[35] A. L. Hodgkin and A. F. Huxley, J. Physiol. (London) **117**, 500 (1952).
[36] R. FitzHugh, Biophys. J. **1**, 445 (1961).
[37] J. Nagumo, S. Arimoto, and S. Yoshizawa, Proc. IRE **50**, 2061 (1962).
[38] For a review of calculations using the IF model, see A. N. Burkitt, Biol. Cybern. **95**, 1 (2006); **95**, 97 (2006).
[39] D. J. Amit and M. V. Tsodyks, Network **2**, 259 (1991).
[40] B. Ermentrout, Neural Comput. **6**, 679 (1994).
[41] O. Shriki, D. Hansel, and H. Sompolinsky, Neural Comput. **15**, 1809 (2003).
[42] Y. Aviel and W. Gerstner, Phys. Rev. E **73**, 051908 (2006).
[43] M. Oizumi, Y. Miyawaki, and M. Okada, J. Phys. Soc. Jpn. **76**, 044803 (2007).
[44] B. Lindner and L. Schimansky-Geier, Phys. Rev. Lett. **86**, 2934 (2001).
[45] A. Renart, R. Moreno-Bose, X.-J. Wang, and N. Parga, Neural Comput. **19**, 1 (2007).
[46] J. Heinzle, P. König, and R. F. Salazar, Cognit. Neurodynamics **1**, 225 (2007).
[47] A. Riehle, S. Grün, M. Diesmann, and A. Aertsen, Science **278**, 1950 (1997).
[48] S. C. de Oliveira, A. Thiele, and K. P. Hoffman, J. Neurosci. **17**, 9248 (1997).
[49] P. Fries, J. H. Reynolds, A. E. Rorie, and R. Desimine, Science **291**, 1560 (2001).
[50] A. D. Reyes, Nat. Neurosci. **6**, 593 (2003).
[51] F. Grammont and A. Riehle, Biol. Cybern. **88**, 360 (2003).
[52] P. H. E. Tiesinga and T. J. Sejnowski, Neural Comput. **16**, 251 (2004).
[53] H. Risken, *The Fokker-Planck Equation: Methods of Solution and Applcation* (Springer, Berlin, 1992).